Canopy Structural Modeling Based on Laser Scanning

Zoltán Vekerdy, Patrick van Laake, Joris Timmermans and Remco Dost

International Institute for Geo-Information Science and Earth Observation
P.O.Box 6, 7500 AA Enschede, the Netherlands
Email: vekerdy@itc.nl, vanlaake@itc.nl, j_timmermans@itc.nl *and* dost@itc.nl

ABSTRACT

A terrestrial laser scanning (TLS) experiment was carried out in the EAGLE 2006 campaign to characterize and model the canopy structure of the Speulderbos forest. Semi-variogram analysis was used to describe spatial variability of the surface. The dependence of the spatial variability on the applied grid size showed, that in this forest spatial details of the digital surface model are lost in the case of larger than 0.3-0.4 m grid size. Voxel statistics was used for describing the density of the canopy structure. Five zones of the canopy were identified according to their density distribution. Basic geometric structures were tested for modeling the forest at the individual tree level. The results create a firm basis for modeling physical processes in the canopy.

INTRODUCTION

Light detection and ranging (LIDAR) or laser scanning uses optical wavelengths to measure distances. Sensors are used from ground-based or airborne platforms for a large variety of applications. With this technology, very complex surfaces and structures can be mapped with a high level of detail in a relatively short time. Reference [1] gives a recent review about the technology and the geometric aspects. Besides industrial applications, there are few standard products produced routinely, like DTMs, but in spite of the fast development in sensor technology, operational applications are lagging behind.

A typical application group, among others, is the characterization of the surface topographically as well as the description of the geometry of land cover, like built-up areas [2] or vegetated environments, including forests [3]. In several cases, the vegetation-caused inaccuracies in terrain reconstruction are mentioned without an analytical approach to vegetation structure, i.e. the vegetation is a source of noise [4]. Vegetation canopy is not completely opaque to the laser beam, because the energy is scattered back from different leaves, branches or even the ground, resulting in a temporally distributed backscatter. Full waveform vertical sampling in large footprint LiDARs uses this for deducing information about the vegetation cover [5, 6]. The profiles of the backscattered energy are highly correlated with estimated above-ground biomass [7]. Discrete return airborne LiDARs, or small footprint LiDARs provide single point information, with a larger density than the large footprint sensors. The point cloud over a unit area, which contains sufficient number of samples, can provide information about the vertical distribution of the canopy, allowing estimates of forest volume and biomass, even in multi-layered canopies with different levels of undergrowth [8, 9].

Terrestrial laser scanning (TLS) provides useful information about the structure of the forest [10, 11]. It can be used for tree-level forest mensuration data extraction [12]. Comparison of field data (stem location, tree height, stem diameter at breast height (DBH), stem density, and timber volume) with point clouds collected from different vantage points showed in different pine and mixed forest sites that TLS demonstrates promise for objective and consistent forest metric assessment, but further work is needed to refine and develop automatic feature identification and data extraction techniques. Correspondingly, the literature contains several examples for stem and branch modeling, e.g., [13]. All these attempts are made to support classical forester aims, i.e. to describe parameters, which are related to timber production and fire management [14, 15].

Wind speed attenuation is related to the cumulative leaf area along the wind path into the canopy [16]. Laser scanning was proved to be effective in leaf area index determination [17]. In fact, not only the leaves but all the branches and stems, i.e. the canopy structure affects the wind, which is an important factor in the surface energy balance.

Laser scanning, both airborne and terrestrial, results is enormous data sizes (point clouds) even from relatively small plots. At the recent stage of technology, they can be useful in the direct inventory of forests with limited sizes, but seem

unsuitable for fulfilling the vast information needs of forest managers. Therefore, more generic methods are needed based on more synoptic methods, e.g. “classical” optical remote sensing. Detailed geometric information about experimental sites allows the detailed modeling of the radiation conditions above and below the complex canopy, leading to the understanding of geometric dependence of backscattering and absorption of energy by the canopy, i.e., developing remote sensing methods for forest inventory. Furthermore, characterization of canopy structure may lead to better understanding of physical processes at the air-surface interface, which affect the energy balance.

The objective of this study is to describe forest canopy structure in detail to support physical remote sensing methods.

MEASUREMENT SETUP

During the EAGLE 2006 campaign, terrestrial laser scanning data was collected from a Douglas fir stand around the Speulderbos observation tower at 52°15’08.1” N, 05°41’25.8” E, 52 m. a.m.s.l. This forest was planted in 1962. In 2006, the average tree density was 785 tree ha^{-1}, with an average tree height of 32 m.

A Leica HDS 2500 pulse scanner was used in the experiment, which has a 6 mm footprint at 50 m. Its single point range accuracy is ±4 mm, the angular accuracy is ±60 μrad.

Completeness of forest scanning highly depends on the location of the sensor. Chasmer et al. compared the laser return percentiles of TLS and ALS, and found that the terrestrial method provides more return from the lower levels of the canopy, whilst the airborne method gives higher return from the top of the canopy [12]. A substantial part of the canopy is excluded from both: the upper parts of the canopy from the TLS and the lower parts of the canopy from ALS, due to the obstruction by objects closer to the sensor. To minimize obstruction, several scanning locations were used around the selected plot: three on the ground and five at different heights (8, 16, 22, 32 and 42 m above ground level) from the elevator of the Speulderbos observation tower (Fig. 1). The top scanner location was about 10 m higher than the average canopy top level and about 7 m higher than the tallest tree.

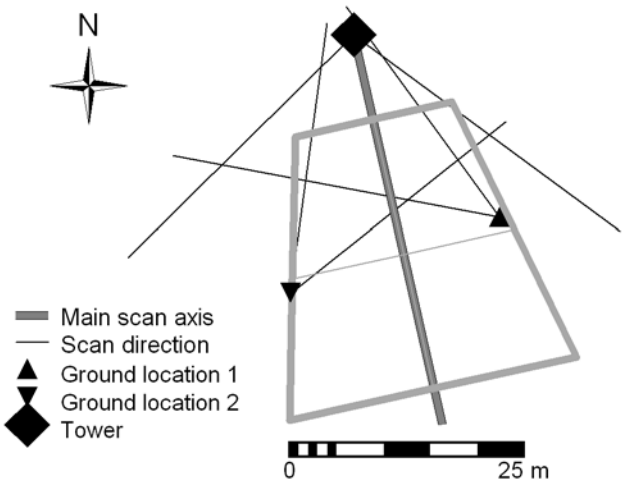

Fig. 1 Experimental setup

In the first step of the processing, the point clouds of the different measurements were co-registered and merged. Then the analysis focused on the best represented region, see grey box in Fig. 1.

DIGITAL SURFACE MODEL OF THE TOP OF THE CANOPY

Digital surface models (DSM) were created with different grid sizes, varying from 0.05-0.9 m, as the bounding surface of the highest point of each grid cell. The variogram surface of the finest grid showed that the DSM is isotrop, proving that the original spatial pattern of the the trees planted rows were supressed by the time, most probably due to forest cultivation and natural competition for light.

The semi-variogram of the digital surface model is spherical. After a regular increase to the sill (range of the fitting variograms vary between 4 and 4.2 m), a very slight periodicity is observable with approximately 8-9 m wavelength. This is related to the average distance between trees. To define field biomass, stems with a DBH > 0.1 m were counted on ten 500m^2 plots in the neighbourhood of the scanned area. The average number of stems is 32.2 per plot, or 644 per hectare, which gives an average spacing between the trees of 4.45m.

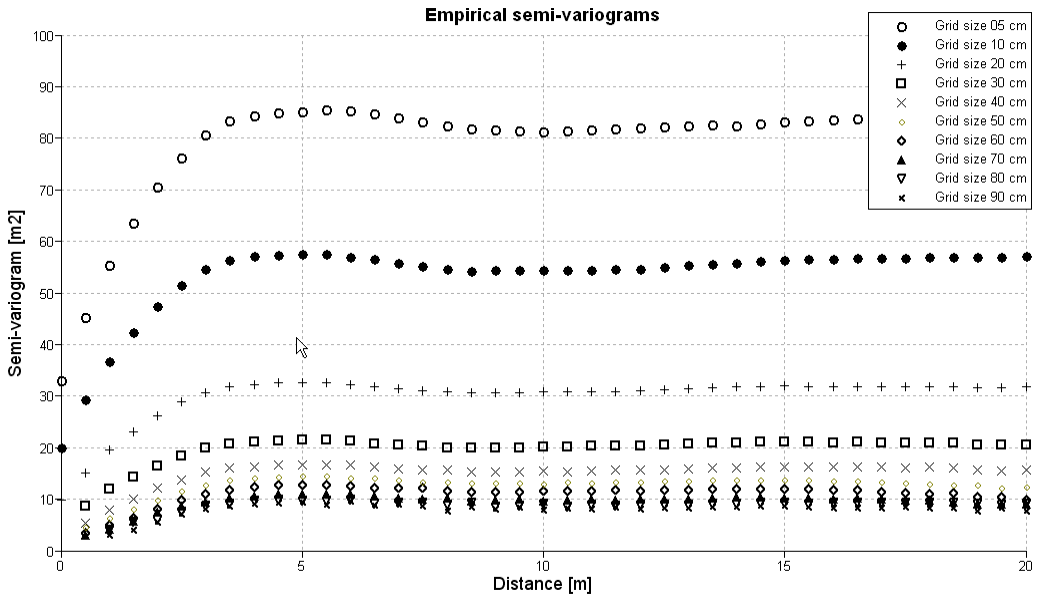

Fig. 2 Semi-variograms calculated from grids of different resolutions

Spatial variance of the variable is characterized with the sill. In the examined part of the Speulderbos forest (matured Douglas fir) it changes according to a negative exponential function with the increasing grid size (Fig. 3).

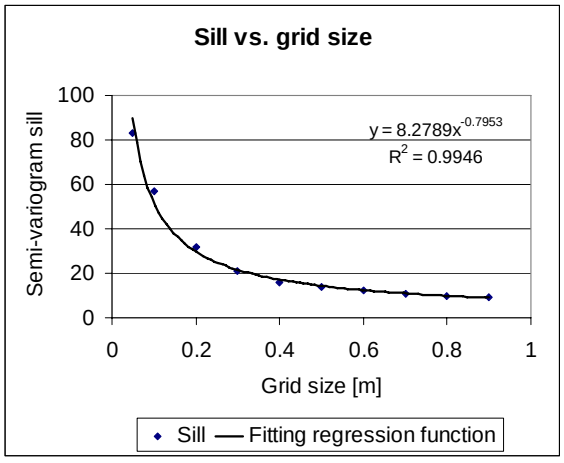

Fig. 3 Change of the sill as a function of the grid size

Note that the parameters of the above regression equation is very much site-specific. It suggests that in this case a grid size larger than 0.4-0.5 m results in a smoothing of the surface, i.e. in the loss of details. This information is used in the further analysis.

CANOPY DENSITY

Resistance against air flow (wind) is a function of canopy density. It is best described as the number of unit volumes (voxels) occupied by solid parts of the canopy (leaves, branches, stems), i.e. canopy voxels, related to the total volume of the canopy, which includes voids as well (Eq. 1).

$$DC = f\frac{\sum VC}{\sum V} \quad \text{Eq. 1}$$

Where *DC* is the density of the canopy, *f* is a scaling factor, *VC* refers to a canopy voxel, i.e., a voxel with laser-reflecting material and *V* is any voxel within the canopy, including the voids.

In the analysis, a linear voxel size of 0.1 m was used, assuming that the variance of the size of the solid particles of the canopy is still well described with it. The variogram analysis (see above) has also supported this assumption. To avoid multiple counting of reflecting elements, only two types of voxels were identified: canopy voxel, which contains solid reflecting canopy elements, and void voxel, which does not contain reflecting canopy elements. For calculating statistics, voxels were ordered in 1 m thick horizontal layers and 1 m thick vertical sections, normal to the main scan axis (Fig. 1). In the following, we shall use the term 'layer segment' to that part of a layer which falls in a vertical section.

The vertical distribution of the canopy density in the experimental site should be calculated according to Eq. 1. Unfortunately, the detection of each canopy voxel is impossible due to limited visibility of certain remote regions hidden by obstructing objects closer to the sensor. Therefore, it was assumed that a normalized density, i.e. the number of detected canopy voxels in a layer segment related to the total number of detected canopy voxels in the corresponding vertical section represents the vertical density distribution (Eq. 2). Similar approach (percentile distribution of the laser returns) was proved to allow the comparison of different measurements throughout a plot in 3D [11].

$$D_i = f\frac{\sum_j VC_{i,j}}{\sum_i \sum_j VC_{i,j}} \quad \text{Eq. 2}$$

Where D_i is the normalized density, *f* is a scaling factor, VC refers to a canopy voxel, *i* refers to the horizontal layers and *j* refers to the vertical sections. The result for the studied forest plot is shown in Fig. 4.

Five basic zones of the Speulderbos canopy can be identified:

- Ground level, which includes the ground and some low vegetation and litter on its surface (layer 1; 0-1 m), resulting in high (virtual) density, and the zone up to 6 m, which is characterized with relatively few and small branches. The relative density is low, but it is increasing by the elevation.
- Medium density zone (7-14 m), with constant density.
- Transitional zone (14-18 m) with increasing density.
- High density zone (19-27 m), where most of the leaves and branches can be found, taking advantage of access to light. This zone of the strongest intersection between the trees.
- Canopy top zone (28-35 m), where the trees do not reach each other. This zone is represented by the DSM. The relative density diminishes by the increasing elevation.

These different zones represent different resistances against wind.

The calculated relative densities depend on the thickness of the sampled volume, i.e. the depth of the sampled area along the main scan axis (Fig. 1). The analysis of the sensitivity of the relative densities to the sample thickness revealed that in this forest, sampled volumes with more than 7-8 metres may represent well the vertical density distribution, since the density values do not show much variance in most of the layers (Fig. 5).

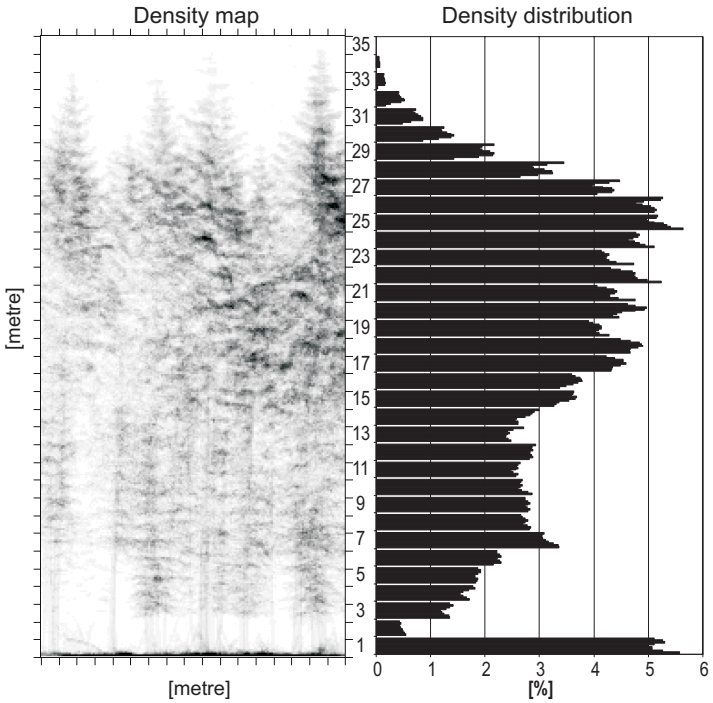

Fig. 4 Density distribution of the forest canopy

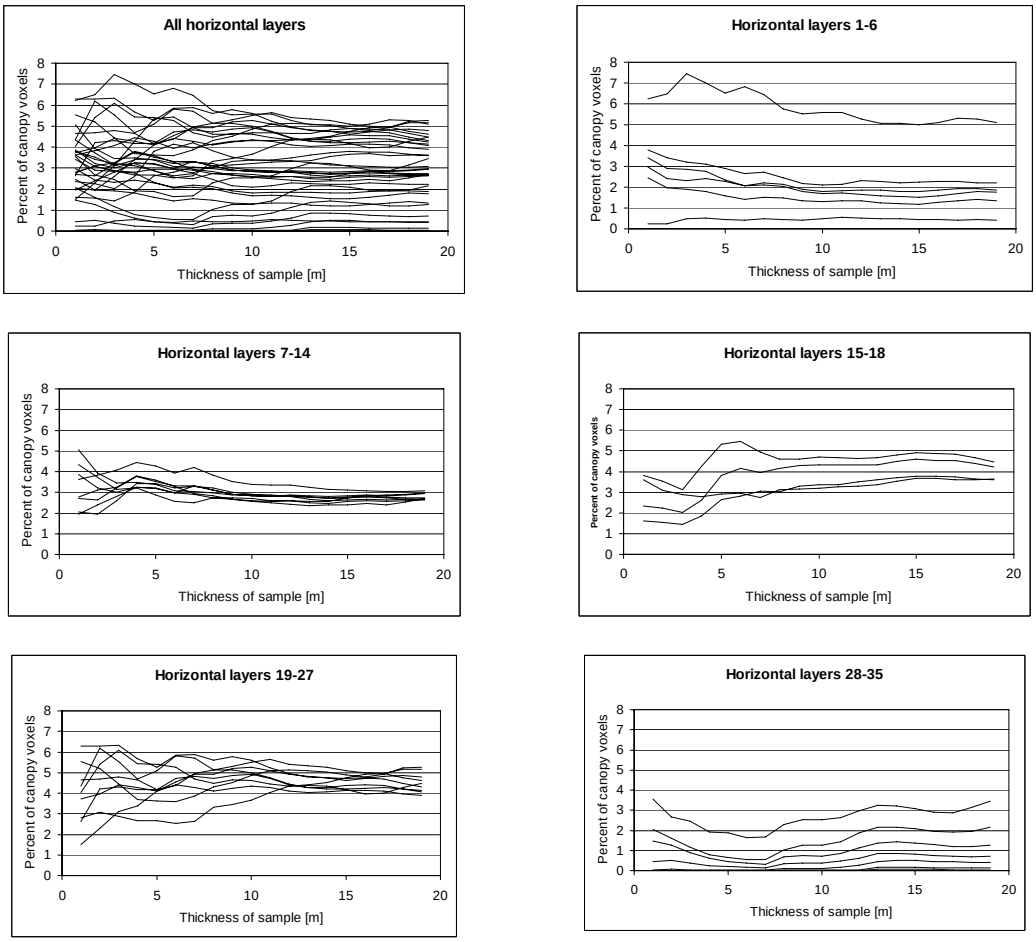

Fig. 5 Change of canopy density as a function of the sample thickness

FOREST MODEL

Traditionally, tree volume is calculated by measuring the girth at about 1.30 meter above the ground (diameter at breast height, DBF), and possibly some other parameters such as height of the first branch or base of the canopy, and then applying these measurements to a previously developed allometric equation. One of the fundamental problems with allometric equations is that they are empirical and lump all aspects of tree physiology into one metric. As environmental conditions change (e.g. soil type, elevation, radiative environment, climate, incidence of pests) the accuracy of the allometric equation degenerates.

The use of lidar data can be a highly accurate method for the determination of tree volume and thus aboveground biomass, but other physical properties of the tree can be assessed as well. Previous research has looked at the accurate measurement of stem girth and height, bifurcation of stem and branches and canopy volume [4, 5]. Such properties of the canopy are directly applicable to various types of more advanced allometric equations, but they also have application in biophysical models of forest dynamics.

Here we are trying to construct a conformal volumetric geometry representing the volume of the canopy. (Conformality here refers to volume of the canopy.) For the pine trees in the study area the cone is the most appropriate geometry, but ellipsoids or cylinders may be used for other types of trees in a similar fashion. What all volumetric geometries have in common is that they are defined by two parameters, in the case of the cone being the base diameter and the height from base to top. Rather than using all the returns from a single tree we here opted for the generalization of the point cloud into a fine raster of maximum elevation which is then contoured to identify the parameters (Fig. 6). This greatly simplifies the procedure, given that the crowns of the trees interact due to the small distance between specimens. The contours are then fitted to circles, which in turn are fitted to a cone, extending from the top of the tree to the level where the crowns of adjacent trees start to overlap. In Fig. 6, crosses indicate calculated locations of the top of the cone. Note that these are not always in the center of the center contour due to the fitting of the cone to all contours of the tree. Distance between the trees is from 3.5 to 8 meter. Clearly visible are also two gaps in the canopy on the top-right and left sides of the figure.

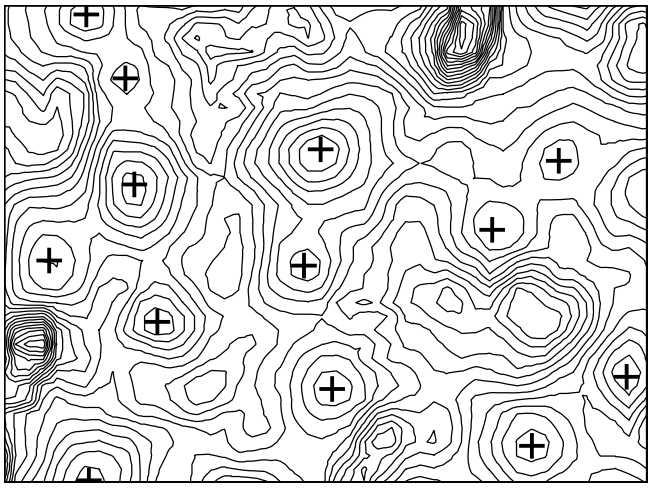

Fig. 6 Contours with 1 meter vertical resolution from DSM resampled to 50 cm raster resolution

Fitting the contours to a cone involves several steps that can be controlled by the analyst. The resampling interval of the original laser data is typically the most influential. Resampling at a large interval produces clean data, but this comes at the cost of detail (Fig. 7), both in the plane and vertically. The best resolution does not always give the best results, though. Fitting the smoother contour at lower resolution to a circular section of a cone is much easier, that is to say that it can be done with lower residual error, than with data at the highest possible resolution. Where the canopies are freestanding, fitting the contours to a circle yielded a goodness-of-fit 0.92 at 50 cm, reducing to 0.64 at 30 cm, to a hardly workable 0.12 at 10 cm sampling resolution.

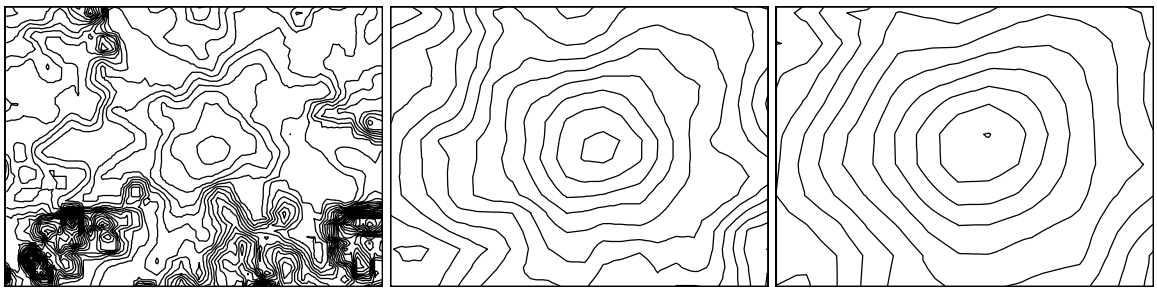

A B C

Fig. 7 A single tree sampled at 10 cm, 30 cm, and 50 cm, respectively. The contours can be fitted to circles with an average goodness-of-fit of 0.12, 0.64, and 0.92, respectively. Other than the obvious loss in planar detail there is also a loss of vertical resolution.

In a second step the circular sections derived from the contours have to be fitted to a conformal cone. While this is relatively straightforward from a purely geometrical perspective, the situation is here compounded by the skew in the center points of the conic sections. This skew, which is in the order of 0.40 to 1.60 meters, can partially be attributed to the natural development of the trees, partly to wind shear. Here we assumed that the skew does not significantly affect the volume of the canopy and we have therefore aligned the circles on their center points. Conformality is now easily achieved by summing the volume of conic cross-sections defined by adjacent conic planar sections and reducing the resultant volume to base radius and height.

Intersection of the canopies of neighbouring trees can be solved in a variety of ways. We have here used as indicator the goodness-of-fit of fitting the contours of the canopy to planar cross-sections of the cone: where the first derivative of the goodness-of-fit is decreasing the canopy is assumed to start interacting with nearby canopies. This assumes that the canopy interaction height is isotropic in the forest stand, which would imply a constant spacing of the trees. While this is not the case in most natural forests, as in Speulderbos, we have found this to be a reasonable, objective indicator of canopy intersection. Below the intersection the canopy is assumed to have a cylindrical form down to the base of the canopy.

CONCLUSIONS

An accurate assessment of the volume and surface of the canopy has many applications in forest modeling. The bi-directional reflectance distribution function (BRDF), canopy closure, surface roughness, and other physical properties can be derived from the ensemble of geometrical shapes making up the forest [18-20]. In addition, interaction of radiation and the forest is mostly through the canopy. This is most obvious for photosynthesis, but heat exchange is also largely controlled by stomatal action in the canopy. As such, the representation of the forest canopy in a series of geometrical shapes can contribute significantly to the development of models of forest dynamics. For model calibration and validation, further analysis and measurements are planned, e.g. to define the light and wind distributions in and above the canopy.

ACKNOWLEDGEMENTS

The EAGLE 2006 campaign made this experiment possible. The measurements were made by FUGRO Inpark B.V. Special thanks to Erik Claassen, for data pre-processing and support during the analysis. Many members of the ITC EAGLE field team contributed directly or indirectly to the success of the campaign.

REFERENCES

[1] Pfeifer, N. and C. Briese. *Geometrical aspects of airborne laser scanning and terrestrial laser scanning*. in *Proceedings of the ISPRS Workshop 'Laser Scanning 2007 and SilviLaser 2007'*. 2007. Espoo, Finland, ISPRS, ASPRS, Finnish Geodetic Institute and Helsinki University of Technology: 311-319.

[2] Vosselman, G., B.G.H. Gorte, G. Sithole and T. Rabbani. *Recognizing structure in laser scanner point clouds*. in *Proceedings of Conference on Laser scanners for Forest and Landscape assessment and instruments*. 2004. Freiburg, Germany: 33-38.

[3] Hyyppä, J., H. Hyyppä, P. Litkey, X. Yu, H. Haggrén, *et al. Algorithms and methods of airborne laser scanning for forest measurements*. in *Proceedings of the ISPRS working group VIII/2 'Laser-Scanners for Forest and Landscape Assessment'*. 2004. Freiburg, Germany, Institute for Forest Growth, Institute for Remote Sensing and Landscape Information Systems, Albert Ludwigs University 82-89.

[4] Töyrä, J. and A. Pietroniro, *Towards operational monitoring of a northern wetland using geomatics-based techniques.* Remote Sensing of Environment, 2005. **97**(2): 174-191.

[5] Lim, K., P. Treitz, M. Wulder, B. St-Onge and M. Flood, *LiDAR remote sensing of forest structure.* Progress in Physical Geography, 2003. **27**(1): 88-106.

[6] Skowronski, N., K. Clark, R. Nelson, J. Hom and M. Patterson, *Remotely sensed measurements of forest structure and fuel loads in the Pinelands of New Jersey.* Remote Sensing of Environment, 2007. **108**(2): 123-129.

[7] Drake, J.B., R.O. Dubayah, R.G. Knox, D.B. Clark and J.B. Blair, *Sensitivity of large-footprint lidar to canopy structure and biomass in a neotropical rainforest.* Remote Sensing of Environment, 2002. **81**(2-3): 378-392.

[8] van Aardt, J.A.N., R.H. Wynne and R.G. Oderwald, *Forest volume and biomass estimation using small-footprint lidar-distributional parameters on a per-segment basis.* Forest Science, 2006. **52**(6): 636-649.

[9] Maltamo, M., P. Packalen, X. Yu, K. Eerikainen, J. Hyyppa, *et al.*, *Identifying and quantifying structural characteristics of heterogeneous boreal forests using laser scanner data.* Forest Ecology and Management, 2005. **216**(1-3): 41-50.

[10] Pfeifer, N. and D. Winterhalder. *Modelling tree cross sections from terrestrial laser scanning data with free-form curves*. in *Proceedings of the ISPRS working group VIII/2 'Laser-Scanners for Forest and Landscape Assessment'*. 2004. Freiburg, Germany, Institute for Forest Growth, Institute for Remote Sensing and Landscape Information Systems, Albert Ludwigs University: 76-81.

[11] Chasmer, L., C. Hopkinson and P. Treitz. *Assessing the three-dimensional frequency distribution of airborne and ground-based LIDAR data for red pine and mixed decidious forest plots*. in *Proceedings of the ISPRS working group VIII/2 'Laser-Scanners for Forest and Landscape Assessment'*. 2004. Freiburg, Germany, Institute for Forest Growth, Institute for Remote Sensing and Landscape Information Systems, Albert Ludwigs University: 66-70.

[12] Hopkinson, C., L. Chasmer, C. Young-Pow and P. Treitz, *Assessing forest metrics with a ground-based scanning lidar.* Canadian Journal of Forest Research, 2004. **34**: 573-583.

[13] Watt, P.J. and D.N.M. Donoghue, *Measuring forest structure with terrestrial laser scanning.* International Journal of Remote Sensing, 2005. **26**(7): 1437-1446.

[14] Morsdorf, F., E. Meier, B. Kotz, K.I. Itten, M. Dobbertin, *et al.*, *LIDAR-based geometric reconstruction of boreal type forest stands at single tree level for forest and wildland fire management.* Remote Sensing of Environment, 2004. **92**(3): 353-362.

[15] Mitsopoulos, I.D. and A.P. Dimitrakopoulos, *Canopy fuel characteristics and potential crown fire behavior in Aleppo pine (Pinus halepensis Mill.) forests.* Annals of Forest Science, 2007. **64**(3): 287-299.

[16] Daudet, F.A., X. Le Roux, H. Sinoquet and B. Adam, *Wind speed and leaf boundary layer conductance variation within tree crown - Consequences on leaf-to-atmosphere coupling and tree functions.* Agricultural and Forest Meteorology, 1999. **97**(3): 171-185.

[17] Hosoi, F. and K. Omasa, *Voxel-based 3-D modeling of individual trees for estimating leaf area density using high-resolution portable scanning lidar.* IEEE Transactions on Geoscience and Remote Sensing, 2006. **44**(12): 3610-3618.

[18] Peddle, D.R., F.G. Hall and E.F. LeDrew, *Spectral mixture analysis and geometric-optical reflectance modeling of boreal forest biophysical structure.* Remote Sensing of Environment, 1999. **67**(3): 288-297.

[19] Gastellu-Etchegorry, J.P., P. Guillevic, F. Zagolski, V. Demarez, V. Trichon, *et al.*, *Modeling BRF and radiation regime of boreal and tropical forests: I. BRF.* Remote Sensing of Environment, 1999. **68**(3): 281-316.

[20] Guillevic, P. and J.P. Gastellu-Etchegorry, *Modeling BRF and radiation regime of boreal and tropical forest: II. PAR regime.* Remote Sensing of Environment, 1999. **68**(3): 317-340.